Global chemical weathering dominated by continental arcs since the mid-Paleozoic

Thomas M. Gernon[a,*], Thea K. Hincks[a], Andrew S. Merdith[b], Eelco J. Rohling[c], Martin R. Palmer[a], Gavin L. Foster[a], Clément P. Bataille[d], R. Dietmar Müller[e]

[a] *School of Ocean & Earth Science, University of Southampton, Southampton SO14 3ZH, UK*
[b] *Laboratoire de Géologie, Université of Lyon 1, France*
[c] *Research School of Earth Sciences, The Australian National University, Canberra, Australia*
[d] *Earth and Environmental Sciences, University of Ottawa, Ottawa, ON K1N, Canada*
[e] *EarthByte Group, School of Geosciences, The University of Sydney, Australia*

Extended Data Figures and Tables

This PDF file includes:

Extended Data Figures 1–8

Extended Data Tables 1–2

Please note that any associated references are provided in the Methods section of the main manuscript

*Corresponding author: Thomas.Gernon@noc.soton.ac.uk

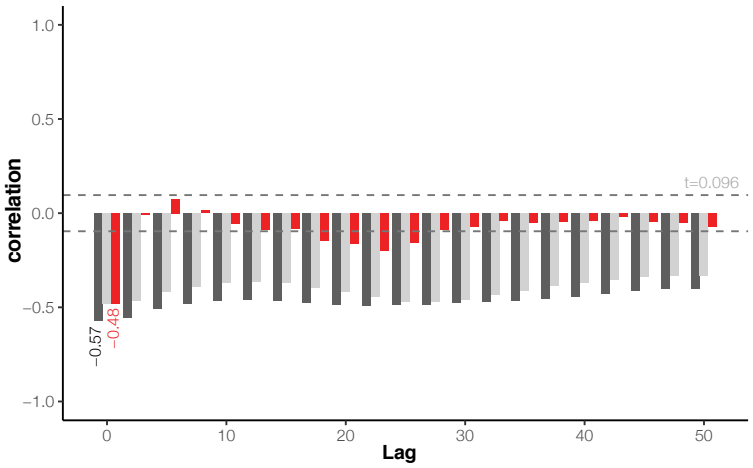

Extended Data Figure 1. Relationship between seawater Sr composition and atmospheric CO_2 since 410 Ma | Bar plot showing the empirical rank correlation (Spearman's rank correlation, in dark grey), BN rank correlation (modelled, light grey), and BN conditional rank correlation (modelled, red) for pCO_2 and $(^{87}Sr/^{86}Sr)_{sw}$ at lags from 0 to 50 Myr. Here, the conditional rank correlation is the correlation between the two variables at a given lag, accounting for the effects of all shorter lags—similar in principle to the multivariate partial autocorrelation. The horizontal dashed lines denote 99% confidence intervals (t = 0.096).

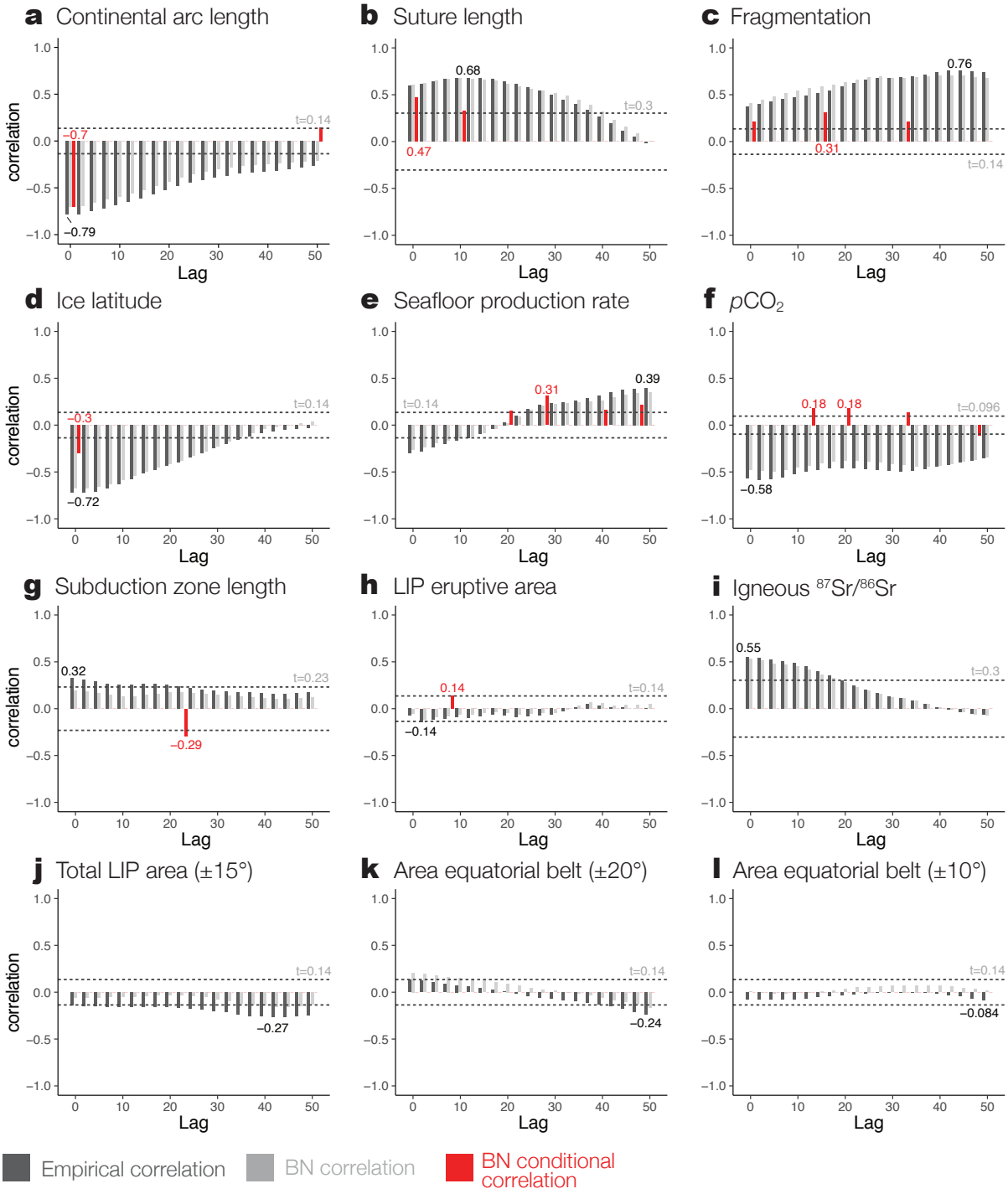

Extended Data Figure 2. The correlations of geologic processes with $(^{87}Sr/^{86}Sr)_{sw}$ and their time lags | The plots show the empirical rank correlations (C_{Emp}), Bayesian Network correlations (C_{BN}), and BN conditional rank correlations (C_{Cond}), at time lags from 0 to 50 Myr in 5 Myr intervals. The values shown in grey on the plots are the highest value of C_{Emp}, and those in red are the peak C_{Cond}. The thresholds for the 99% confidence intervals (t) are shown with horizontal dashed lines.

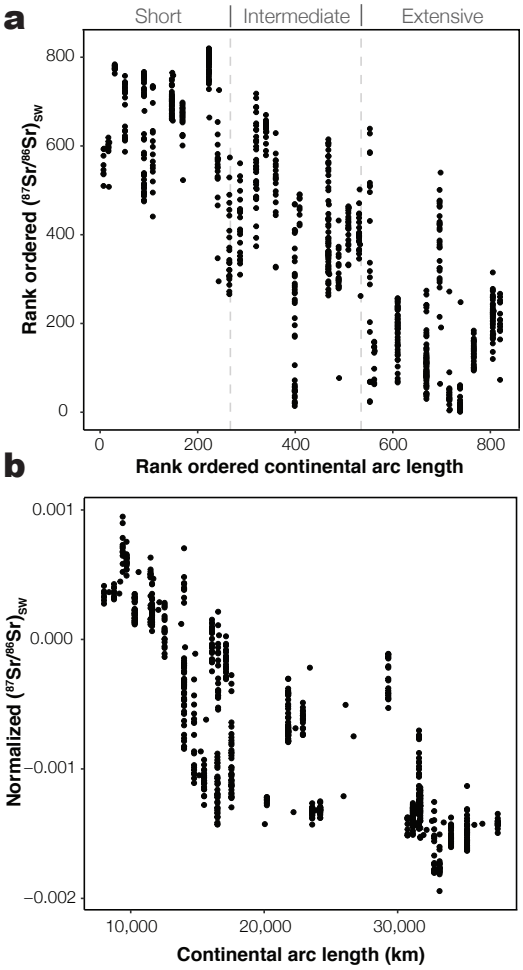

Extended Data Figure 3. Relationship between continental arc length and the strontium isotopic composition of seawater | a, Ranked $(^{87}Sr/^{86}Sr)_{sw}$ versus ranked continental arc length; note that the dashed vertical lines show the division between short (<16,100 km), intermediate (16,100–29,300 km), and extensive (≥29,300 km) arc systems, as shown in Fig. 2a (these divisions denote approximately equal quantiles); **b,** Unranked (parametric) normalised $(^{87}Sr/^{86}Sr)_{sw}$ (using ref.[13]) versus unranked continental arc length (see Fig. 2a for the ranked version of this plot).

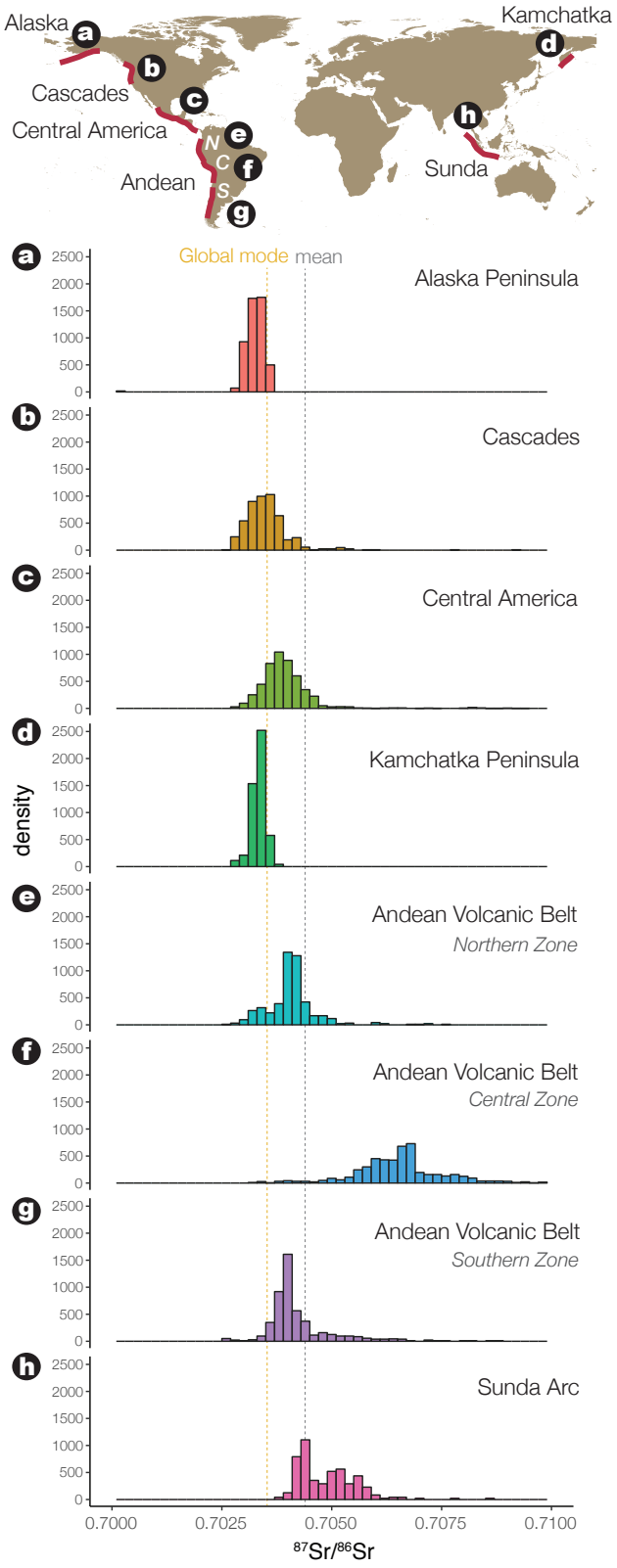

Extended Data Figure 4. (Continued on the following page.)

Extended Data Figure 4. (preceding page) **Present-day global distribution of continental volcanic arcs, and their Sr isotope compositions |** Map of continental volcanic arcs identified by Cao et al.[14]). The labels (A–H) correspond to the density histograms, which show the relative frequency of $^{87}Sr/^{86}Sr$ points for each arc from the EarthChem Library (earthchem.org). The mean and mode of the dataset (total N=5498) are represented by vertical dashed lines. Note that the relatively high $^{87}Sr/^{86}Sr$ compositions of the Central Zone of the Andean Belt can be explained by the presence of extremely thick crust in this region (>70 km) and a higher degree of crustal assimilation[63].

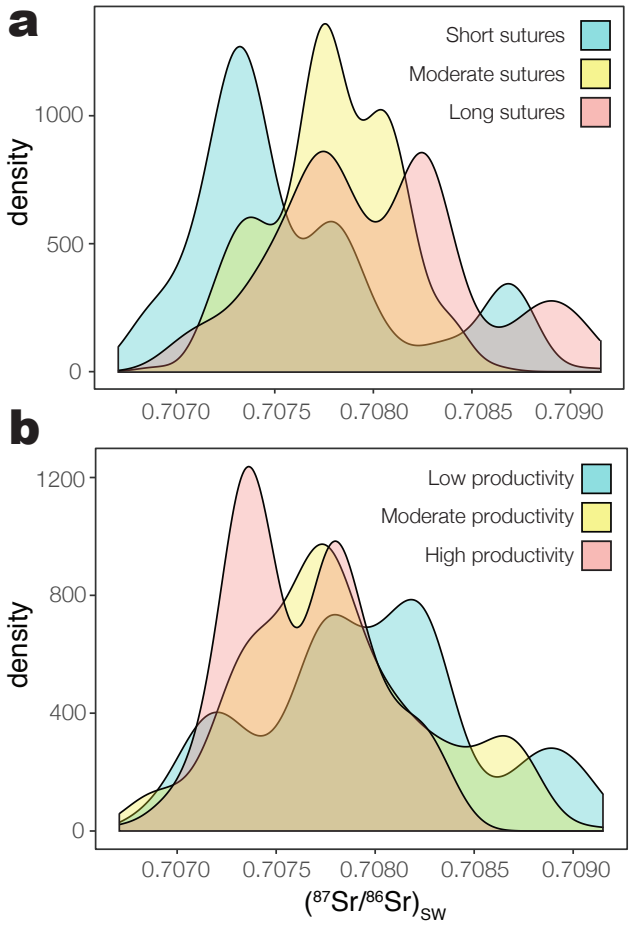

Extended Data Figure 5. Effects of suture zones and seafloor production rates on the strontium isotopic composition of seawater | Probability density for **a,** suture zone length[5], identifying short (<5,180 km), intermediate (5,180–9,730 km), and long (≥9,730 km) suture zones (note that these divisions are approximately equal quantiles); and **b,** seafloor production rates, discriminating low (<3.96 km^2 yr^{-1}), moderate (3.96–4.95 km^2 yr^{-1}) and high (>4.95 km^2 yr^{-1}) production rates.

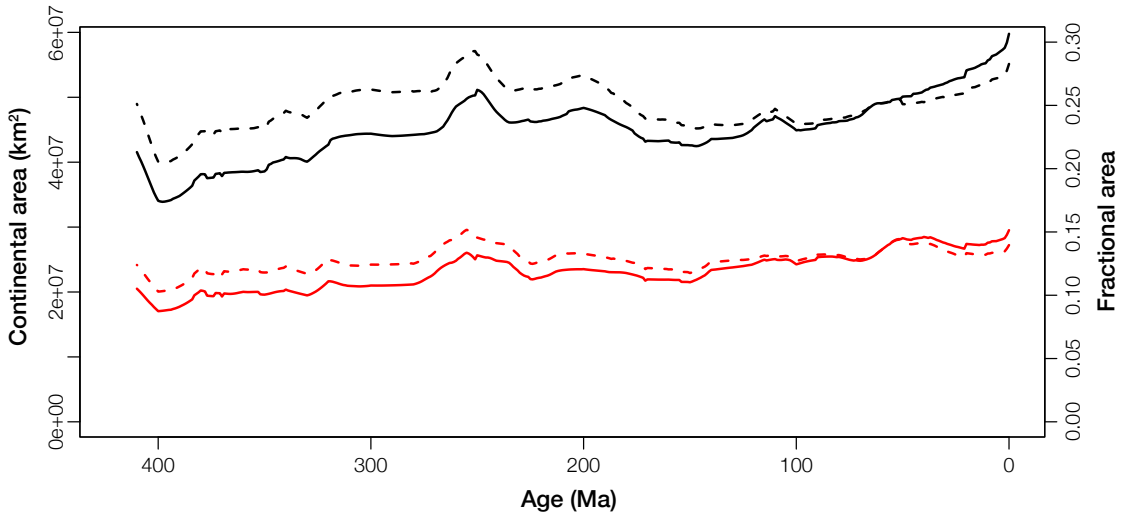

Extended Data Figure 6. Clustering of continents within the tropics since 400 Ma | Solid lines show the continental area within 20° (black) and 10° (red) of the equator through time, using the paleomagnetic reference frame of Domeier and Torsvik[54], as extracted from Matthews et al.[11]. The dashed lines show the fractional area (i.e., area within the belt divided by the total crustal area) through time. The source data are provided in Supplementary Data File S1.

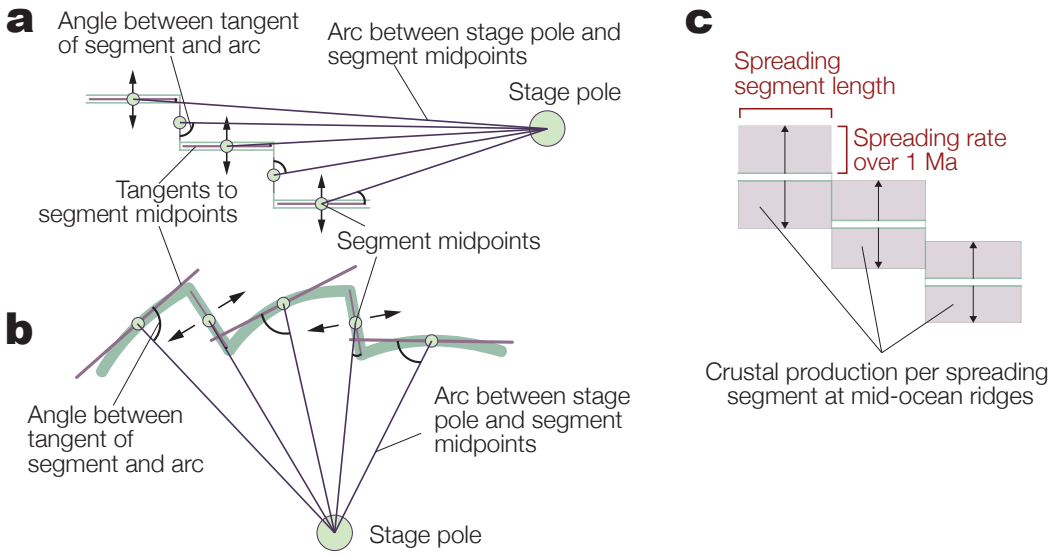

Extended Data Figure 7. Calculation of seafloor production at mid-ocean ridges | Diagram explaining the formal quantification of seafloor production rates (Methods). In *GPlates*, mid-ocean ridges contain both spreading and transform segments. **a,** and **b,** show how we distinguish these segments. Each mid-ocean ridge line is broken into separate segments. We take the mid-point of each segment and draw the tangent to it. In some cases this matches the segment quite well (e.g., **a**) and in other cases the segment is more curved (e.g., **b**). We then draw a great circle from the stage pole that describes the motion of one ridge flank from the other, to the mid-point of the segment. We then calculate the deviation angle between these two lines. As transform segments should form small circles around the stage pole, their deviation angle should be large, whilst the deviation angle for spreading segments should be small. We found 70° was a reasonable cut off, though in some locations where spreading is poorly constrained or very oblique, it does not work completely. Once we distinguished the spreading and transform segments, we extract the full spreading velocity of each segment **c,** and multiply this by the length of the ridge segment to calculate the crustal production.

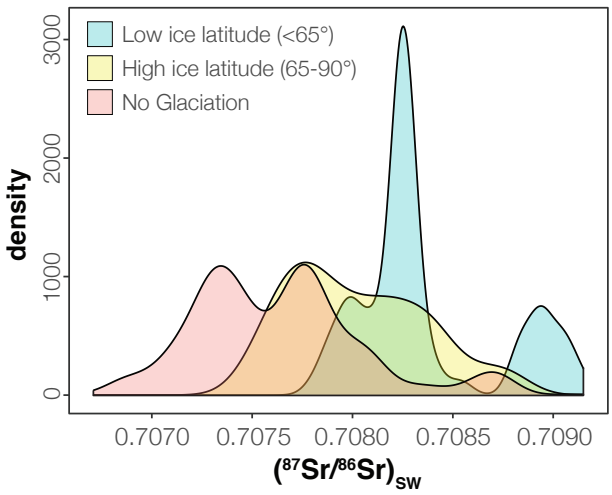

Extended Data Figure 8. Effects of latitudinal ice extent on the strontium isotopic composition of seawater | Probability density for ice latitudinal extent (see key). The distributions show that more extensive (i.e., severe) glaciations favor high $(^{87}Sr/^{86}Sr)_{sw}$, and vice versa.

Extended Data Table 1: Correlation matrix for all nodes in our final Bayesian Network with $(^{87}Sr/^{86}Sr)_{sw}$. Note that C_{Emp} = Empirical Rank Correlation; C_{BN} = BN Rank Correlation; C_{Cond} = Conditional Rank Correlation; Av = Average value over the specified time lag interval (if this is not specified the interval is 0 Myr; i.e. no lag). Nodes with C_{Cond} greater than the 99 percent confidence interval threshold (CI_{thresh}, see the Methods for further details) were retained in the BN and are shown here. The reader is directed to Supplementary Data File S2 (2020-10-18246_S2.xlsx) for the full table of correlations that includes nodes that were subsequently eliminated from the BN.

Node	$\mathbf{C}_{Emp}$	$\mathbf{C}_{BN}$	$\mathbf{C}_{Cond}$
Continental Arc Length	-0.787	-0.700	-0.700
Suture Zone Length	0.592	0.606	0.468
Ice Latitude	-0.719	-0.678	-0.299
Fragmentation	0.374	0.408	0.214
LIP Eruptive Area Av 7.5 Myr	-0.110	-0.084	0.139
Suture Zone Length Av 10 Myr	0.678	0.673	0.327
pCO_2 Av 12.5 Myr	-0.496	-0.430	0.180
Fragmentation Av 15 Myr	0.513	0.582	0.308
pCO_2 Av 20 Myr	-0.457	-0.381	0.182
Seafloor Production Av 20 Myr	0.029	0.021	0.151
Subduction Length Av 22.5 Myr	0.238	0.177	-0.292
Seafloor Production Av 27.5 Myr	0.220	0.206	0.312
Fragmentation Av 32.5 Myr	0.681	0.674	0.212
pCO_2 Av 32.5 Myr	-0.493	-0.429	0.136
Seafloor Production Av 40 Myr	0.319	0.265	0.168
Seafloor Production Av 47.5 Myr	0.391	0.343	0.216
pCO_2 Av 47.5 Myr	-0.380	-0.371	-0.110
Continental Arc Length Av 50 Myr	-0.267	-0.208	0.146

Extended Data Table 2: Empirical rank correlation matrix (C_{Emp}) for $(^{87}Sr/^{86}Sr)_{sw}$, normalised $(^{87}Sr/^{86}Sr)_{sw}$, and $^{87}Sr/^{86}Sr$ of igneous (ign.) rocks through time[16]. Note that the data used to calculate C_{Emp} in this table span the interval from 1–360 Ma (i.e., to allow a direct comparison with those using time lags, Extended Data Table 1), and that no time lags are included here.

Node	**$(^{87}Sr/^{86}Sr)_{sw}$**	**N$(^{87}Sr/^{86}Sr)_{sw}$**	**Ign. $^{87}Sr/^{86}Sr$**
Continental arc length	-0.787	-0.819	-0.704
Suture zone length	0.592	0.395	0.378
Ice latitudinal extent	-0.719	-0.561	-0.624
Land area, tropics (±20°)	0.134	-0.085	0.022
Land area, tropics (±10°)	-0.074	-0.409	-0.341
Fragmentation index	0.374	-0.007	-0.099
Subduction zone length	0.325	0.529	0.660
Seafloor production rates	-0.303	-0.282	-0.510
pCO_2	-0.571	-0.401	-0.225
LIP weatherable area (±15°)	-0.139	-0.535	-0.403
LIP eruptive area	-0.074	-0.341	-0.358
Igneous $^{87}Sr/^{86}Sr$	0.554	0.738	1.000
N$(^{87}Sr/^{86}Sr)_{sw}$	0.716	1.000	0.738
$(^{87}Sr/^{86}Sr)_{sw}$	1.000	0.716	0.554